

DESIGN, MANUFACTURING AND VALIDATION OF A GUST GENERATOR FOR WIND TUNNEL TEST OF A LARGE SCALE AEROELASTIC MODEL

Federico Fonte*, **Luca Riccobene***, **Sergio Ricci***,
Stephan Adden** and **Matteo Martegani****

*** Politecnico di Milano**

Department of Aerospace Science and Technology
Via La Masa 34, 20156 Milano, Italy
e-mail: federico.fonte, luca.riccobene, sergio.ricci (@polimi.it)

**** IBK Technologie GmbH & Co. KG/ IBK Innovation GmbH & Co. KG**
Büro Hamburg, Finksweg 2, 21129 Hamburg, Germany

Keywords: *Gust generator, experimental aerodynamics*

Abstract

The paper describes the design, manufacturing and test of a Gust Generator to be installed into the large Wind Tunnel of Politecnico di Milano-Italy (GVPM), used to validate load alleviation technologies implemented into scaled aeroelastic models.

1. Introduction

The need for more efficient aircraft able to meet the new challenging requirements defined by ACARE with its strategic road map stated in the Vision 2020 forces the researchers to look for more advanced aircraft configurations, based on more efficient aerodynamics and structures together with more sophisticated flight control systems. Many of the design approaches nowadays adopted are in some way related to a more flexible wing structure, mainly due to the adoption of more performing materials, such as carbon fiber, and to an aerodynamic design based on higher aspect ratio. On one side more flexible wings allow the designers to implement passive and active technologies for Load Control, meaning the capability to reshape the load distribution aiming at increased aero-structural efficiency. On the other side they

push toward an aggressive combination of maneuver (MLA) and gust load alleviation (GLA) technologies that holds the potential to greatly improve both the weight and aerodynamic terms in the classical Breguet equation. For all these reasons the interest in the development, implementation and experimental verification of MLA and GLA technologies is becoming a key topic in the development of the next generation transport aircraft.

The experimental validation of active control technologies on scaled aeroelastic models is challenging and requires specific equipments in terms of both models and wind tunnel. For these reasons, Politecnico di Milano decided to design and manufacturing a Gust Generator dedicated to the validation of gust load alleviation technologies. Even if this device is of general use, the device has been conceived in the framework of a Cleansky 1 European Project called GLAMOUR, coordinated by Politecnico di Milano. The GLAMOUR project, in response to the SP1-JTI-CS-2013-01-GRA-02-022 call, has two main top level goals. The first one, having the Green Regional Aircraft as reference and adopting the active control laws proposed by the Topic Manager of GRA platform, is to deeply explore their validity over the entire flight envelope. The second one is to extend

them with new control strategies based on the use of Static Output Feedback, Neural Networks, as well as based on Robust Model Predictive Control techniques.

One of the relevant aspect of GLAMOUR project is the extended experimental validation campaign that will be conducted at Wind Tunnel available at Politecnico di Milano. Indeed, the design manufacturing and testing of a large scale aeroservoelastic model for validation of MLA and GLA control strategies requires the adoption of special design and manufacturing technologies due to the restrictions imposed by the scale of the model. One of the most important requirement in terms of experimental setup is the availability of a gust generator able to produce the typical discrete *I-cos* profile requested by the certification rules. This is a challenging task due to the large size of the testing room of POLIMI wind tunnel selected for the test campaign. Indeed, the test room sizes 4x4x6 meters.

3. The Wind Tunnel

The GVPM is a medium size low speed wind tunnel highly dedicated to helicopter and airplane models testing. Due to this facility POLIMI is member of SATA since 2003.

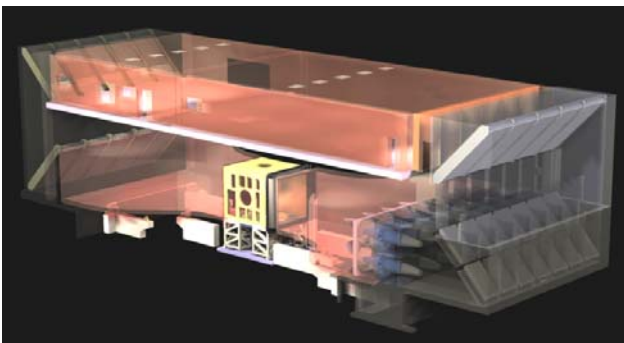


Figure 1: View of the POLIMI's GVPM.

The wind tunnel can operate both in closed test section and in open jet configuration (Figure 1: View of the POLIMI's GVPM.). The closed test section is 6 m long, 4 m wide and 3.84 m high. The first 5 m part of the closed test section is removable to allow for off-line test preparation (or, in case, to allow for open jet tests). Two interchangeable closed test sections

(the "yellow" and the "blue" one) are available (Figure 2). A high flow ratio compressor supplies compressed air for the air bearing movement systems that are used to move the closed test sections and the other heavy structures or machines.

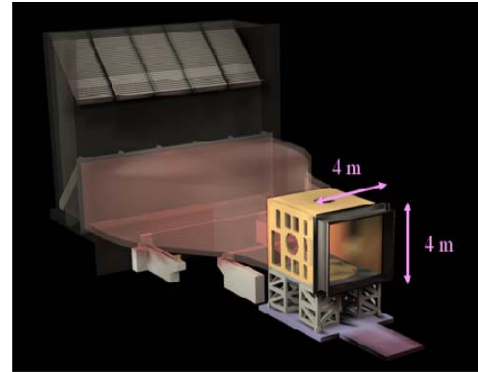


Figure 2: The testing chamber.

The good flow quality is adequate for aeronautical testing (the turbulence level is less than 0.1%). The air flow is produced by 14 fans with a total power of 1.4 MW. By virtue of the heat exchanger, the wind tunnel testing are not affected by any significant temperature gradient so that test duration is not limited by wind tunnel overheating. The wind tunnel is controlled in velocity (from 3 m/s up to 55 m/s). The maximum velocity of 55 m/s corresponds to a maximum Mach number of 0.16 and to Reynolds number per meter of about 3.8 million. As this usually produces a model Reynolds number lower than in the full-scale aircraft, transition strips can be positioned on the model surface. Adhesive tape transition strips are used at GVPM, sized according to NASA TN-3579.

The velocity feedback for the control is obtained by dynamic pressure measurement together with the measurement of thermodynamic quantities necessary to compute the fluid density. The test condition parameters continuously monitored during the test are: dynamic pressure, absolute pressure, absolute temperature and relative humidity. Thus an accurate evaluation of the actual fluid density is possible allowing the flow velocity to be obtained from the dynamic pressure.

2. Gust Generator Requirements

The gust generator device should be able to reproduce the gust disturbance prescribed by the requirements, that is a gust with a I - \cos shape, uniform along the aircraft span and with a defined amplitude. A schematic view of the gust generator is presented in Figure 3, the device is composed by a set of vanes placed at the inlet section of the wind tunnel chamber and the gust velocity that must be generated is directed along the y-axis of the indicate reference system (along the model vertical direction).

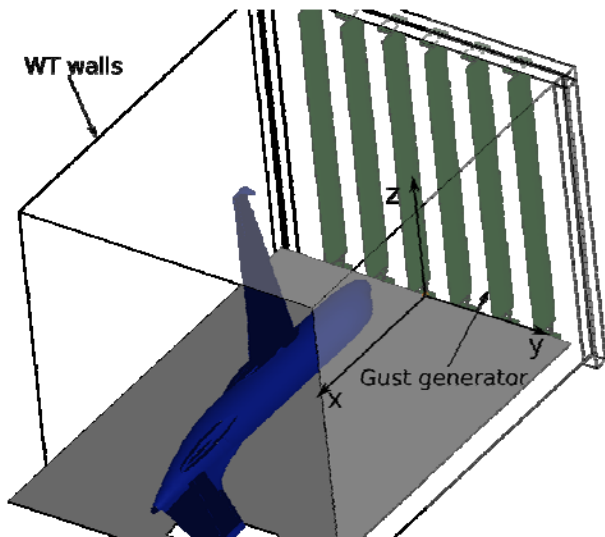


Figure 3: View of the gust generator device inside the wind tunnel chamber.

The values for the required gust angle and frequency were derived from the regulations scaled on the wind tunnel model. In particular four different load conditions were identified, characterized by the gust angle and frequency represented in Table 1. The reduced frequencies of Table 1 have been non-dimensionalized with respect to the reference chord of the wind tunnel model. The preliminary sizing of the gust generator was performed by considering the condition with the highest reduced frequency, that is the second case.

Table 1: Requirements for the gust generator.

	Gust angle [deg]	Reduced frequency
1	4.531	0.0284
2	4.2387	0.0421
3	1.804	0.0227
4	1.704	0.0337

3. Preliminary Sizing

The chosen configuration for the gust generator was defined as a series of vanes with uniform chord and with a NACA 0012 airfoil, placed at the inlet section of the wind tunnel chamber. The vanes rotate around the quarter chord axis in order to impose to the flow a component of velocity in the y-direction of the reference presented in Figure 3. For the actual design of the generator some parameters needed to be fixed, that is the chord of the vanes and the number of vanes, in addition an estimate of the required rotation angle was required.

An increase in the number of vanes could both increase the maximum gust angle and lead to a more uniform gust field in the wind tunnel. On the other hand an increase of the number of the vanes would lead to an increased blockage of the wind tunnel, in addition the flow inside the test chamber would be affected by the several wakes of the vanes. The chord of the vanes is another design parameter, smaller chords would lead to a more lightweight structure, with lower rotational inertia and lower aerodynamic loads acting on them, thus reducing the power requirements of the generator. On the other hand a larger chord would imply also a larger surface of the vanes and again, it will lead to an increase in the gust angle.

In order to assess the influence of the above parameters on the behavior of the gust

generator, and to drive the choice of the final configuration, a series of unsteady 2D CFD simulations were performed, by changing:

- the number of vanes, considering configurations with 2, 6 and 8 vanes;
- the chord of the vanes, considering the values 0.2m, 0.3m and 0.4m;
- the maximum deflection angle, which assumed the values of 6, 9 and 12 degrees.

In order to reduce the computational cost of the numerical analyses, a two-dimensional configuration was considered. This is justified by the fact that the problem is uniform along the z-direction, both in term of geometry and boundary conditions, moreover the region where the gust angle will be studied is located in the middle of the wind tunnel height, and it is assumed that the tip effects of the vanes have a minor influence in that region. The simulations were performed using a mesh with about 110k cells, obtained after a convergence study. The numerical simulation was used to solve the Navier-Stokes equations, along with a Spalart-Allmaras κ - ω turbulence model. An predefined rotation was imposed on the vanes and the ALE scheme was used to solve the equations on the deformed mesh.

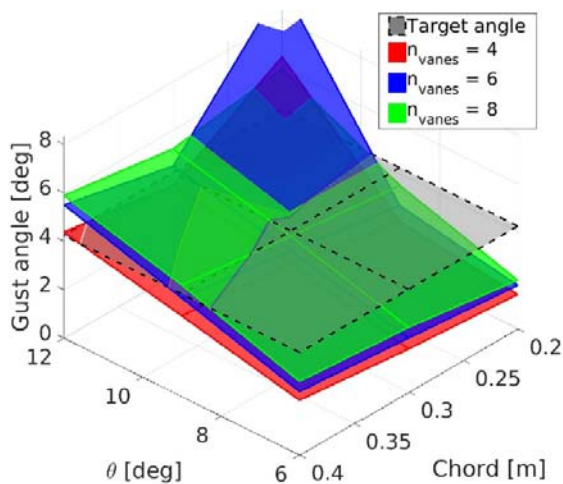


Figure 4: Maximum gust angle obtained for the different configurations.

The results of the numerical simulations are presented in **Figure 4**, while a snapshot of one time response is presented in **Figure 5**. **Figure 4** presents the maximum gust angle obtained for the different configurations, and the plane with dashed borders represents the target angle to be produced. In the figure there is a peak in correspondence of the configurations with smaller chords, when rotated at higher angles, this peak is due to a stall of the airfoils, and thus the corresponding configurations have to be discarded. The onset of stall for the configurations with smaller chord was expected, and it is related to the fact that a decrease in the chord leads to a decrease in both the Reynolds number and the reduced frequency (all the simulation are performed by keeping the same physical frequency). Since a stall would lead to a degradation of the flow in the wind tunnel, the two smaller values of the chord length were discarded. At the same time, there was no need for considering a chord length larger than 0.4m since by using this value the target angle seemed to be achievable, and from the considerations expressed above an increase in the chord length was not desired.

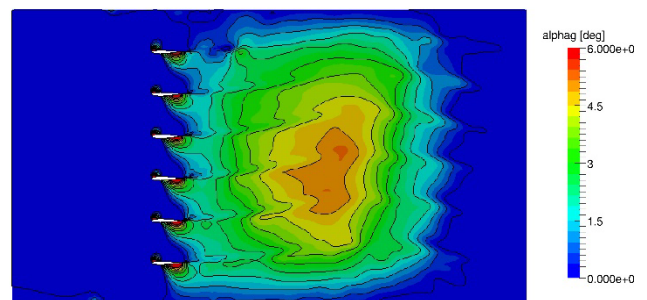


Figure 5: Distribution of the gust angle in the test chamber.

From **Figure 5** it can be seen that, as expected, the gust angle is not uniform inside the wind tunnel, in particular the variation along the z-axis should be limited as much as possible in order to ensure that the different surfaces of the model will encounter the same gust profile during their motion. In order to have numerical estimate of the distribution of the gust angle along the z-axis, the amplitude of the region

where the gust angle is higher than the 90% of the target value was evaluated, the results are presented in **Figure 6**. From **Figure 6** it can be seen that the use of the configuration with 8 vanes leads to a small increase of the amplitude of the gust region with respect to the configuration with 6 vanes and the same behavior could be observed also in the peak value of the gust angle. For this reason the configuration with 8 vanes was discarded and the selected configuration for the gust generator was characterized by the use of 6 vanes with 0.4m chord. The expected maximum deflection angle can be extrapolated from the values in **Figure 4**, obtaining a value of about 9.3° .

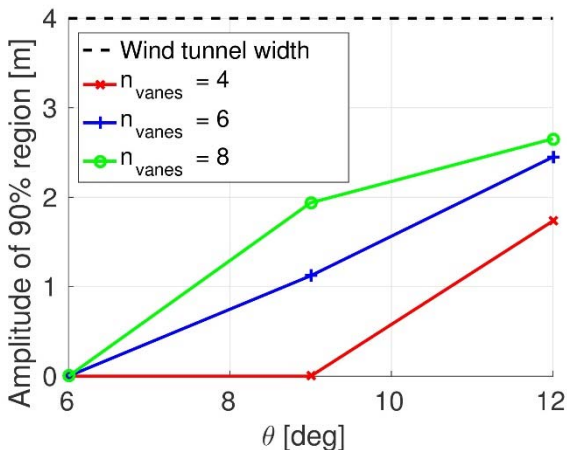


Figure 6: Amplitude of the region where $\alpha_g > 0.9\alpha_{target}$, chord=0.4m.

4. Structural Design

As shown before, the six vanes run from the floor to the ceiling of the test chamber, spanning about 3.8 m, with a chord of 0.4 m; however the actual length is 3.575 m to accommodate for the attachments and the actuation system, located on the wind tunnel floor. The preliminary design of the internal structure took into account different requirements:

- first bending frequency above 15 Hz, thus granting no interference with the wing first modes to be excited, that are below 5 Hz

- deflection under loads below 1% of the vane's span, to limit aeroelastic interactions
- no dynamic instability

Moreover the gust generator system should be easy to install.

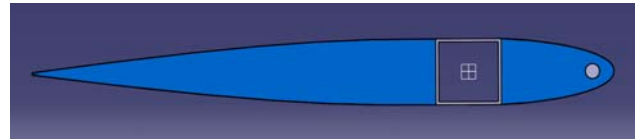


Figure 7: Sketch of the vane's section

As can be seen in **Figure 7**, the load-carrying structure is a square iron tube 45 x 45 mm (with a thickness of 2 mm) placed at 25% of the airfoil chord; attached to this beam are two styrofoam pieces shaped as the leading and trailing edge (the core). The whole vane is covered by a single ply of woven glass fabric E 200 gr twill 2/2, which has the necessary high drapability, since the dry cloth was laid down and the resin applied afterwards. The curing process was conducted at room temperature. The circular steel rod on the leading edge is a static balancing mass and its position is chosen in order to have the center of gravity of the vane as close as possible to the aerodynamic center, thus avoiding dynamic aeroelastic instability, namely flutter.

The choice of the square section was determined by the allowable maximum thickness and to ease the interface with the attachments; in particular the NACA 0012 is slightly modified in order to have the flat surface of the tube connected to the glass fabric: the aerodynamic loads are thus directly transferred to the supporting structure and the core only reproduce the external shape.

Four steel ribs, 2 mm wide, are also welded to the beam and serves as a support for the balancing rod.

The single vane weights about 15 kg and in **Figure 8**, are shown the vanes before the painting.



Figure 8: Vanes before the WT tests

Two modal analyses were conducted: a first one in free-free condition on a single vane, to validate a detailed 3D FEM model and assess the natural frequencies without the connections to the wind tunnel, and a second one on a so called “twin” configuration, i.e. two vanes connected together by the mechanism (see [Figure 9](#)).

In the first setup the 3D FEM model properties were updated to match the free-free natural frequencies. The second setup allowed to verify the actual effect of the connections between the vanes and the wind tunnel. In particular the constraints can be modeled as an hinge (ceiling) since the shaft is connected to an adjustable bearing and as a clamp (floor), where the linear motor that drives the mechanism is active.

28 piezoelectric accelerometers have been placed, 14 on each vane, divided into two columns, with 7 equally spaced rows for each one: 7 accelerometers were placed on the metallic beam (i.e. on the steel beam), while the other sensors were placed close to the trailing edge, to catch torsional modes.

The vanes are free to rotate about their axis, since the actuator is not mounted.

The excitation is given by impact-hammer technique. Frequency response functions were acquired in the range 0-128Hz, with a frequency resolution of 0.125 Hz. Each point was hammered ten times, in order to reduce measuring noise thanks to the averages.

Identification was carried out with software LMS-Test.Lab Rev.13A which uses the

algorithm Polimax. 12 modes were identified until 80Hz.

The first two modes that correspond to the first out-of-plane bending of each vane – obviously a small participation of the other vane is noticeable due to the mechanical link – are respectively 8.47 Hz and 8.81 Hz. While not greater than 15 Hz, these values were deemed acceptable since they're almost two times greater than the natural frequencies of the wing. It was also noted that the attachments do not behave like ideal constraints, explaining the lesser frequencies values obtained.



Figure 9: Twin vanes configuration for modal analysis

A static test was also performed to assess the safety factor, crucial when approaching a wind tunnel test campaign, and to measure the maximum out-of-plane deflection.



Figure 10: Static test on a single vane

As can be seen in **Figure 10**, the setup features the vane in horizontal position, the constraints are the same (hinge – clamp) and the total loads, aerodynamic loads minus weight, are applied using bags filled with lead balls (each one is around 25 kg), that simulate an uniform pressure. The rotation around the beam axis is mechanically inhibited, thus reproducing the motor presence. Two strain gauges are placed at the attachments and three laser sensors are placed at three equally spaced stations along the span.

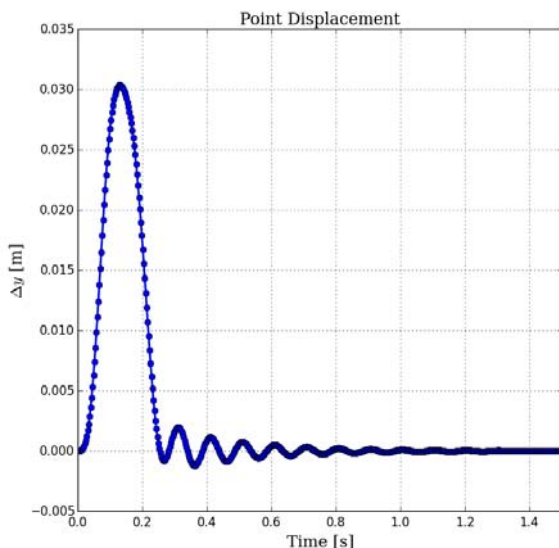


Figure 11: Dynamic response on a single vane given the (1-cos) input: displacement time history at vane half span

The aerodynamic load is estimated with strip theory at a severe condition, 35 m/s and angle of attack of 15° (being 12° the maximum estimated “operational” angle of attack of the vanes): the total aerodynamic load in this condition is 1735 N, which is about two times the loads computed in the previous section with the CFD.

The maximum displacement measured is 42.46 mm at half span, which is 1.2% of the span as prescribed by the design requirements.

Having updated the finite element model with the results of the modal analyses, a reduced order model (beam model) is generated to quickly verify aeroelastic dynamic stability and dynamic response, given the (1-cos) gust input (imposed as a rotation angle time history applied at the attachment with the linear motor). No flutter is found for the test speeds, moreover the dynamic response of the single vane, in terms of maximum nodal displacement, is shown in **Figure 11**.

The maximum rotation imposed is 15° and the simulation is run at 35 m/s.

The maximum displacement due to dynamic loads is 31 mm (at vane's half span), which is an acceptable value.

The simulation is run using MSC NASTRAN: while the structural properties are correlated with the experimental model, the aerodynamic model (doublet lattice) is an approximation of the actual wind tunnel conditions, but represents an upper bound on the dynamic loads acting on the vane.

5. Experimental Validation

The gust generator device was then evaluated at the Large Wind Tunnel at the Politecnico di Milano in order to establish its capabilities and to validate the numerical simulations performed.

The measurements were taken by the use of a three-wire hot wire anemometer, and the test campaign was divided in two parts. In the first part a sensitivity study was performed by measuring the gust angle at a reference point with different deflection angles of the vanes. In the second part of the test campaign a map of

the flow in the wind tunnel was obtained by repeating the measurements in several point in the volume.

The sensitivity study was performed by considering the gust angle at a point located at the coordinates $[2.507, -0.3, 2.0]m$, which correspond to a point in the region that will be occupied by the wing of the wind tunnel model. The sensitivity analysis was repeated for each of the four cases presented in **Table 1**, and the results for the case 2 are presented in **Figure 12**. Since case 2 is also the case considered for the preliminary sizing of the vanes also the numerical results are available and are presented in **Figure 12**.

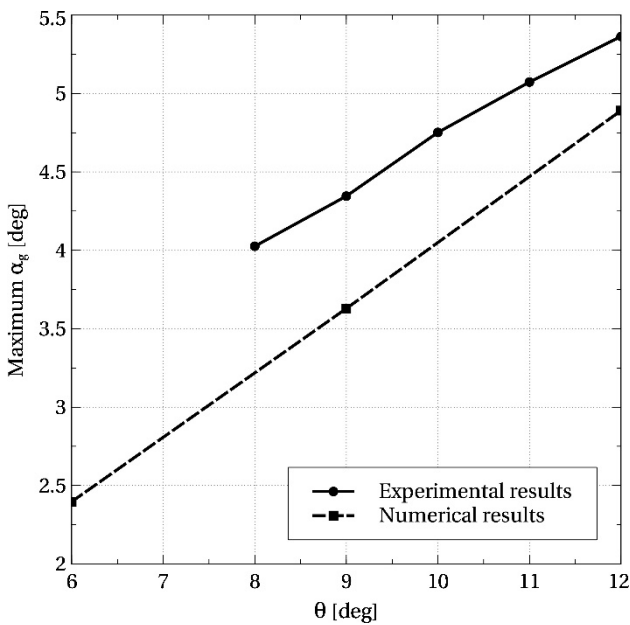


Figure 12: Maximum gust angle for different values of the vanes rotation angle.

The experimental results show a good correlation with the numerical ones. In particular, the required maximum angles have been reached during the wind tunnel tests. **Figure 16** show that the gust peak reaches its maximum close to the vanes, then starting from $x=1.5m$ it remains almost constant along the test chamber showing a limited dissipation.

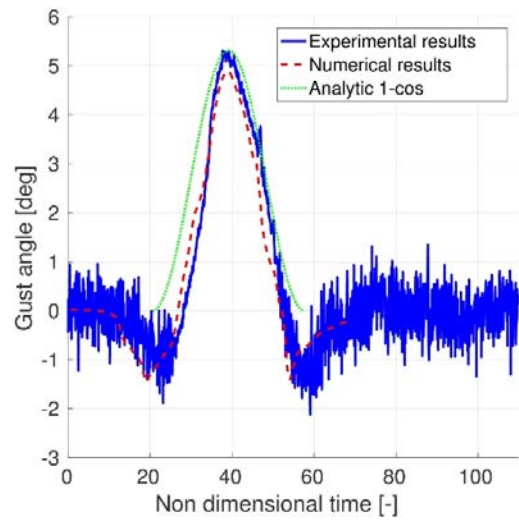


Figure 13: Time history of the gust angle, compared with the numerical results.

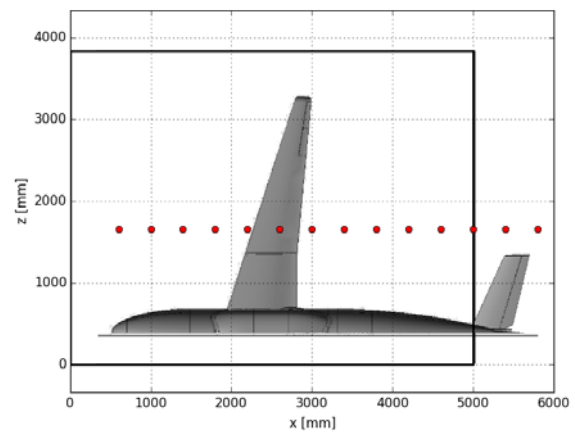


Figure 14: Location of the measurement points with respect to the wind tunnel.

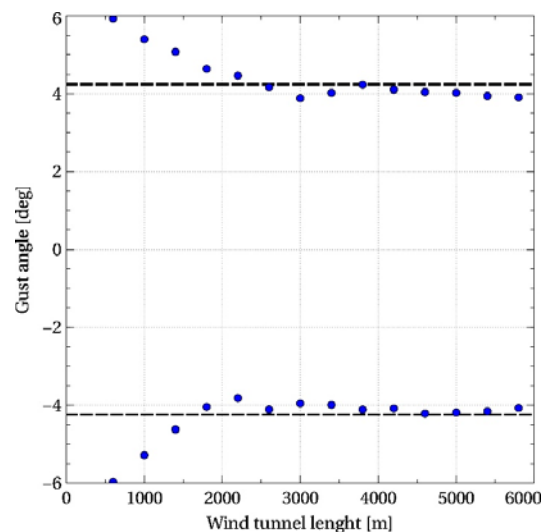


Figure 15: Lengthwise distribution of the gust angle.



Figure 16: The Gust generator installed into the Wind Tunnel.

it as part of their paper. The authors confirm that they give permission, or have obtained permission from the copyright holder of this paper, for the publication and distribution of this paper as part of the ICAS proceedings or as individual off-prints from the proceedings.

6. Conclusions

The paper summarizes the design and manufacturing of a Gust Generator to be installed into the POLMI's large wind tunnel. This device has been conceived to be used during the experimental validation of the gust load alleviation technologies applied on aeroelastic scaled wind tunnel models. The experimental validation campaign demonstrated the validity of the design allowing to reach the gust angles requirements. The device is now installed and ready to be used in the framework of the GLAMOUR EU project.

References

- [1] Work programme 2013 Cooperation Theme 7 Transport (including Aeronautics), European Commission C(2012) 4536 of 9 July 2012..
- [2] European Aeronautics: A Vision for 2020. Group of Personalities. 2001, ISBN 92-894-0559-7.
- [3] ACARE Strategic, Research and Innovation Agenda Vol. 1, Realising Europe's Vision for Aviation, September 2012.
- [4] Fonte, F., Ricci, S., and Mantegazza, P., Gust Load Alleviation for a Regional Aircraft Through a Static Output Feedback, *Journal of Aircraft*, Vol. 52, No. 5, 2015, pp. 1559-1574. Smith J, Jones B and Brown J. *The title of the book*. 1st edition, Publisher, 2001.

Copyright Statement

The authors confirm that they, and/or their company or organization, hold copyright on all of the original material included in this paper. The authors also confirm that they have obtained permission, from the copyright holder of any third party material included in this paper, to publish